

Figure 1

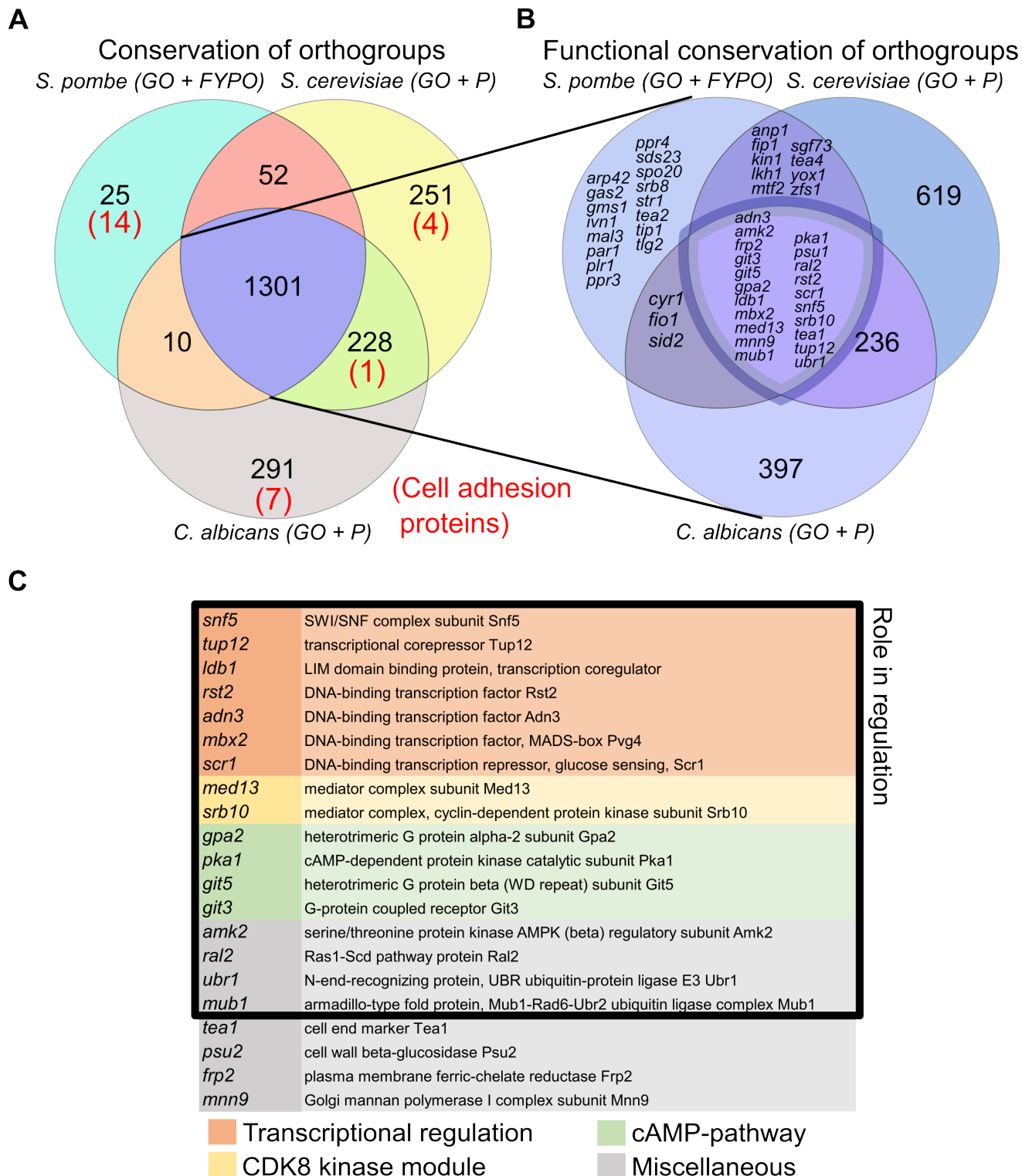


Figure 1: Several regulators of MLP formation are conserved between fission and budding yeast, but cell-adhesion effector proteins are not.
 (A) Venn diagram of numbers of orthogroups, in which at least one gene in the orthogroup is annotated in GO-terms or phenotypic data

related to MLP formation in either *S. pombe*, *S. cerevisiae* or *C. albicans*. Red numbers indicate cell-adhesion proteins. (B) Venn diagram of orthogroups that are conserved across the 3 species (i.e. the middle subset on A) asking whether they are also functionally conserved, i.e. contain at least one gene that is annotated in GO-terms or phenotypic data related to MLP formation in all three species. (C) Functionally conserved genes coloured by their broad functional category as indicated. GO: Gene Ontology, FYPO: Fission Yeast Phenotype Ontology, P: Phenotype annotations.

Figure 2

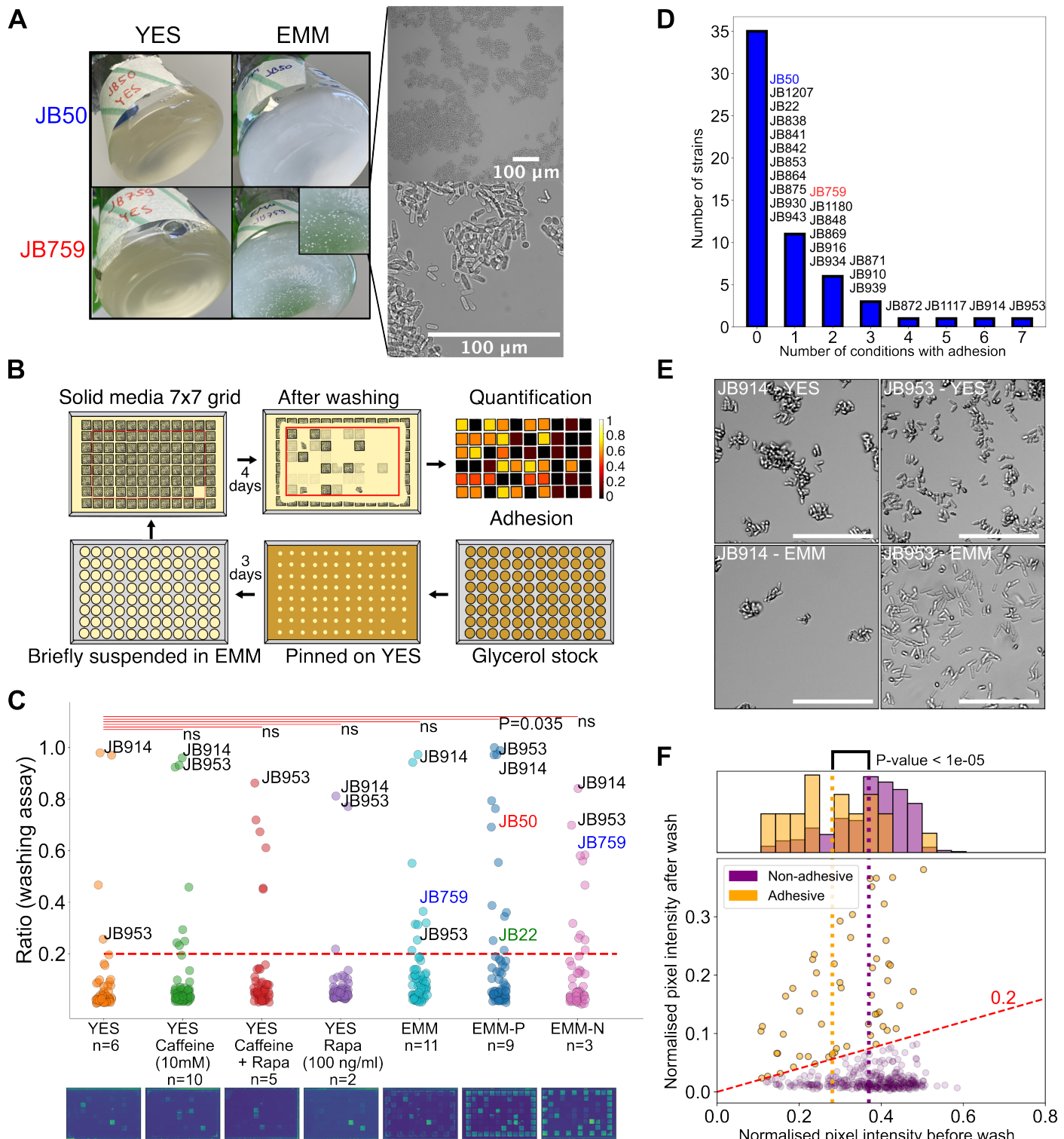


Figure 2: MLP formation in *S. pombe* natural isolates varies with nutrient conditions and is associated with decreased growth. (A) Left: Images of the initial observations on the standard laboratory strain JB50 and the natural isolate JB759 showing MLP formation of JB759 in

EMM. Cells were grown at 32°C for 2 days, shaking at 160 rpm. Right: Microscopy images at two magnifications of the JB759 strain grown in EMM for 2 days. (B) Scheme of the high-throughput adhesion assay used to assess MLP formation in *S. pombe*. (C) Strip plot of adhesion to agar across different conditions in the natural isolate library, with images of representative post-wash agar plates below. Each dot represents the mean adhesion value for a given strain in a specific condition. The red dashed line shows a cut-off for strong phenotypes (intensity after wash >0.2 times than before wash). Each condition was compared to rich media (YES) with the null hypothesis that they do not increase MLP formation. P-values were obtained using a one-sided permutation-based T-test and Bonferroni correction. Comparisons were marked not significant (ns.) where the null hypothesis could not be rejected at significance threshold 0.05. Strains around the edges were not taken into account for any statistical analysis (see Methods). The lab strain JB50 and natural isolate JB759 used in panel (A), as well as the lab strain, JB22, and the highly adhesive strains JB914 and JB953, are highlighted in conditions in which they are adhesive. (D) Histogram showing the number of unique strains forming MLPs in a given number of conditions. (E) Panel of light microscopy images for JB953 and JB914 in EMM and YES, showing representative images of MLP-formation. Scale bars are 100 μm. Rest of the microscopy images from this experiment are displayed in Supplementary Figure 4. Representative images of culture flasks are shown in Supplementary Figure 5. (F) Scatter plot of mean cell densities (measured in normalised inverse pixel intensity) before and after washing. Each dot represents one strain in one condition, orange dots represent adhesive data points (ratio of before-wash to after-wash intensity >0.2, dashed red line) and purple dots represent non-adhesive data points. The histogram shows the distribution of cell densities before washing as a proxy for growth. The vertical dotted orange and purple lines mark the mean pre-wash densities for the two populations.

Figure 3

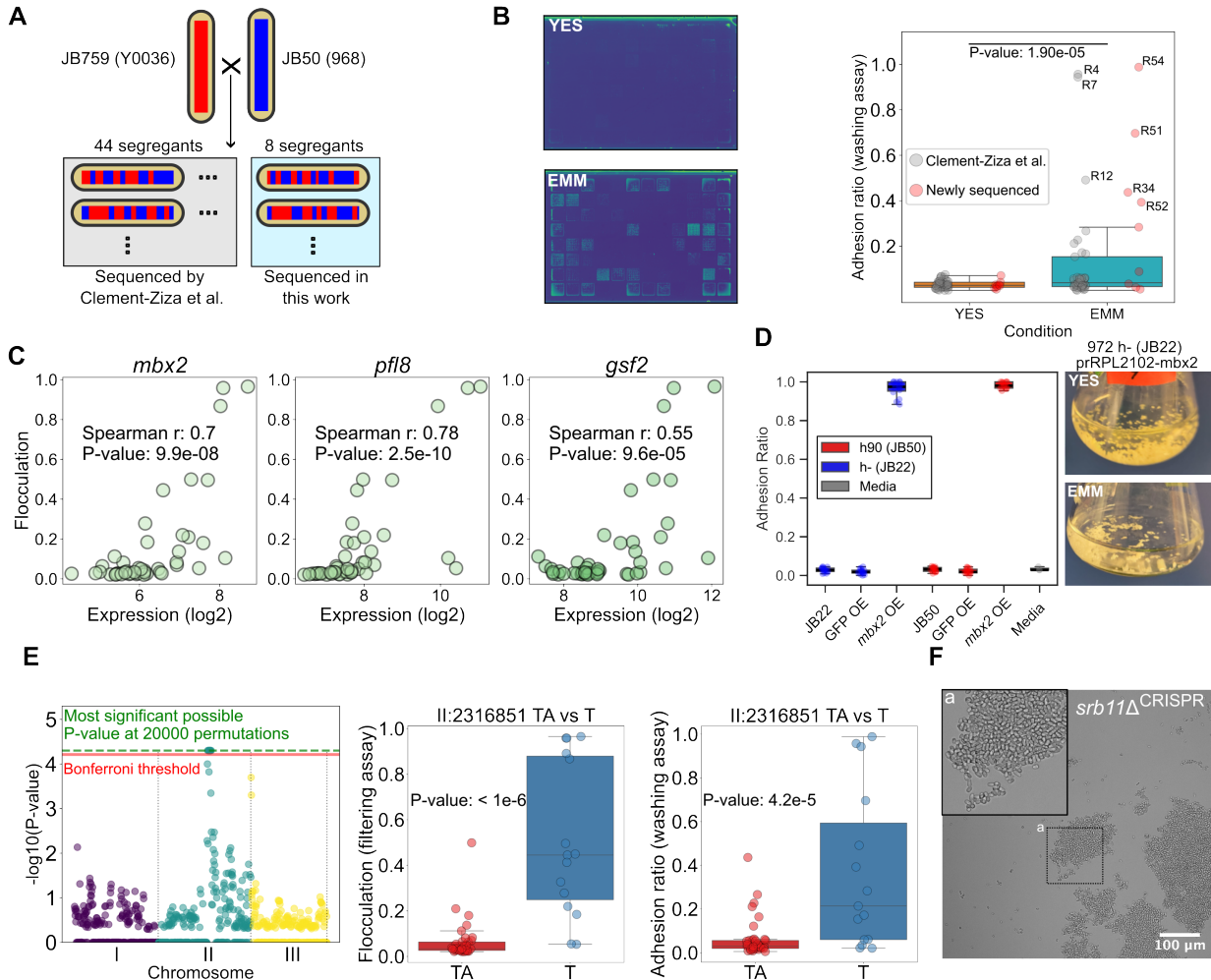


Figure 3: MLP formation in JB759 is driven by *mbx2* expression and associated with a single-nucleotide deletion on chromosome II. (A) Scheme for the JB759xJB50 segregant library. Red and blue stripes indicate genomic recombination resulting from meiosis. SNPs for the strains inside the grey box were previously identified (49) and genome sequencing data for the strains in the light blue box were generated in this work (Methods). (B) (Left) Example plate scans of segregants grown on EMM or YES after washing, shown in viridis colourmap. (Right) Adhesion to agar of segregant strains on EMM (mean of 10 replicates) compared to YES (mean of 2 replicates), along with significance of the difference obtained using permutation-based T-test. (C) Correlations of *mbx2* and flocculin gene expression with flocculation in EMM. Each dot represents a strain from the segregant library. (D) (Left) Box plot of adhesion measurements overlaid comparing adhesion measurements from control, GFP overexpression and *mbx2* overexpression strains in both JB22 and JB50 backgrounds, as well as measurements for empty media (Methods). (Right) Representative images of the flocculating *mbx2* overexpression strain in YES and EMM. Rest of the flask images are found in Supplementary Figure 7B. (E) (Left) Manhattan plot of QTL analysis results for flocculation in EMM. The red line shows the Bonferroni threshold, while the green dashed line shows the highest possible significance achievable using 20,000 permutations. (Middle) Candidate variant II:2316851 TA>T is associated with increased flocculation in EMM (filtering assay, mean of 3 replicates). (Right) Candidate variant II:2316851 TA>T is associated with increased adhesion on EMM (washing assay). P-values determined using a permutation-based T-test with 1E+6 permutations. (F) Microscopy image of *srb11ΔCRISPR* in EMM showing flocculation. The inset shows a close-up of the region highlighted in box "a".

Figure 4

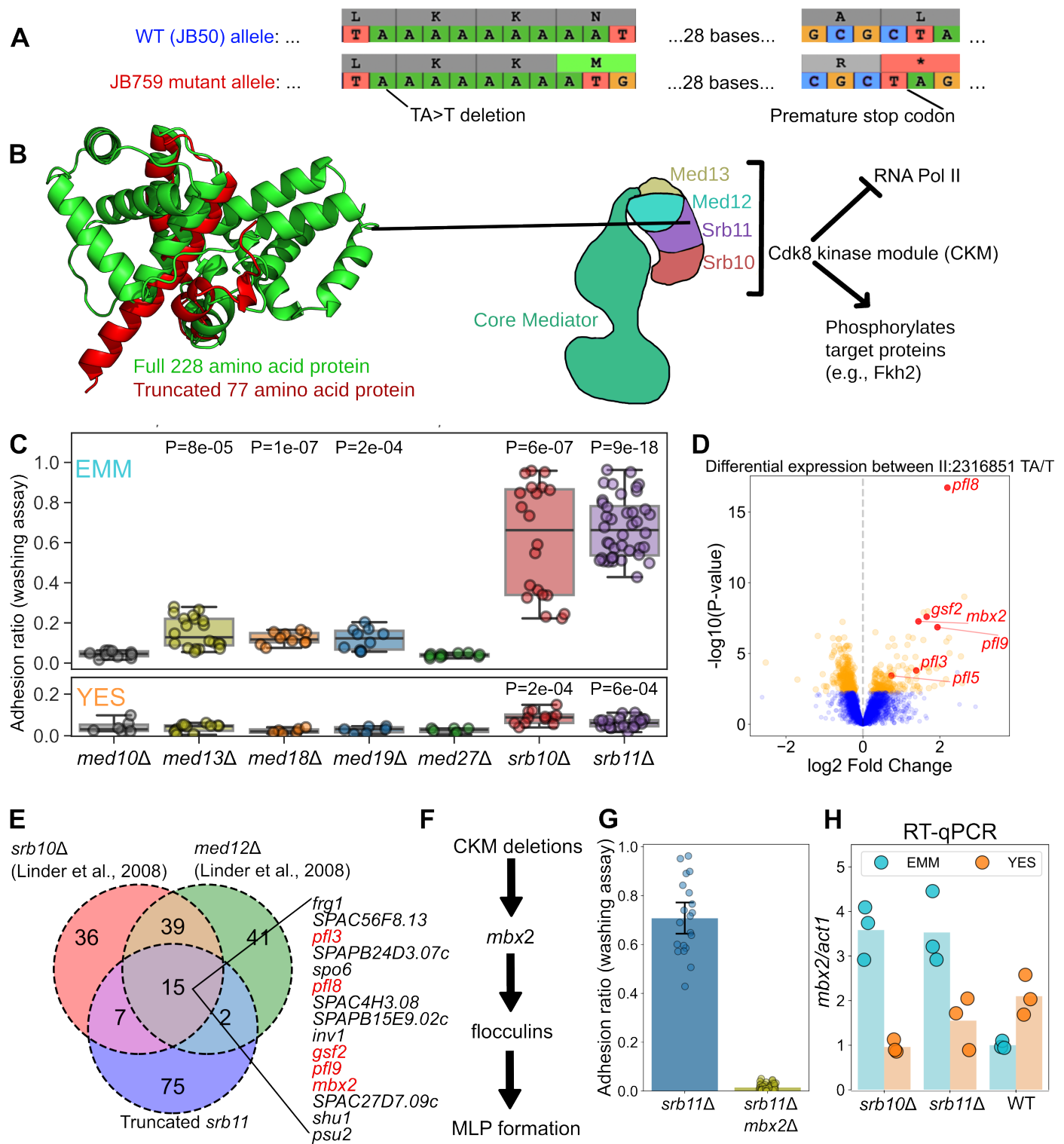


Figure 4: Cdk8 kinase module deletions upregulate *mbx2* in minimal media, but not in rich media, and lead to MLP formation. (A) Scheme showing how a single nucleotide deletion leads to frameshift and premature stop-codon in *srb11*. (B) Full *Srb11* structure (green) compared

with the truncated Srb11 structure (red) as predicted using Colabfold (92). Scheme on the right shows Srb11 in the context of the Cdk8 kinase module of the Mediator complex. The structure was sketched based on structural data (84), and functional roles were summarised based on (84,86). (C) Box plot showing adhesion values from Mediator gene deletion strains from the genome-wide prototrophic deletion library on EMM and YES as indicated. Each dot represents a replicate. P-value represents comparison of each strain against the least adhesive strain in the assay (*med27Δ*) using a T-test. (D) Differential expression analysis of segregant strains split on the II:2316851 TA>T single-nucleotide deletion. Fold-change values and P-values were obtained from DESeq2 (67). Flocculins and *mbx2* are highlighted in red. (E) Overlap of upregulated genes in three CKM mutants based on our *sr11* data and data from Linder et al. (68). (F) Simplified model for how CKM deletions lead to MLP formation. (G) Adhesion measurements for the *sr11Δ* strain obtained from the deletion collection, and its derived strain after *mbx2* knock-out with CRISPR. Each dot represents a replicate measurement. Error bars represent the 95% confidence interval for the mean. (H) RT-qPCR showing *mbx2* expression in JB22 (WT), *sr10Δ::Kan*, *sr11Δ* strains obtained from the genome-wide prototrophic deletion collection in EMM or YES. Expression of each gene is normalised relative to *act1* expression. Height of each bar reflects the mean of three biological replicates which are indicated by dots.

Figure 5

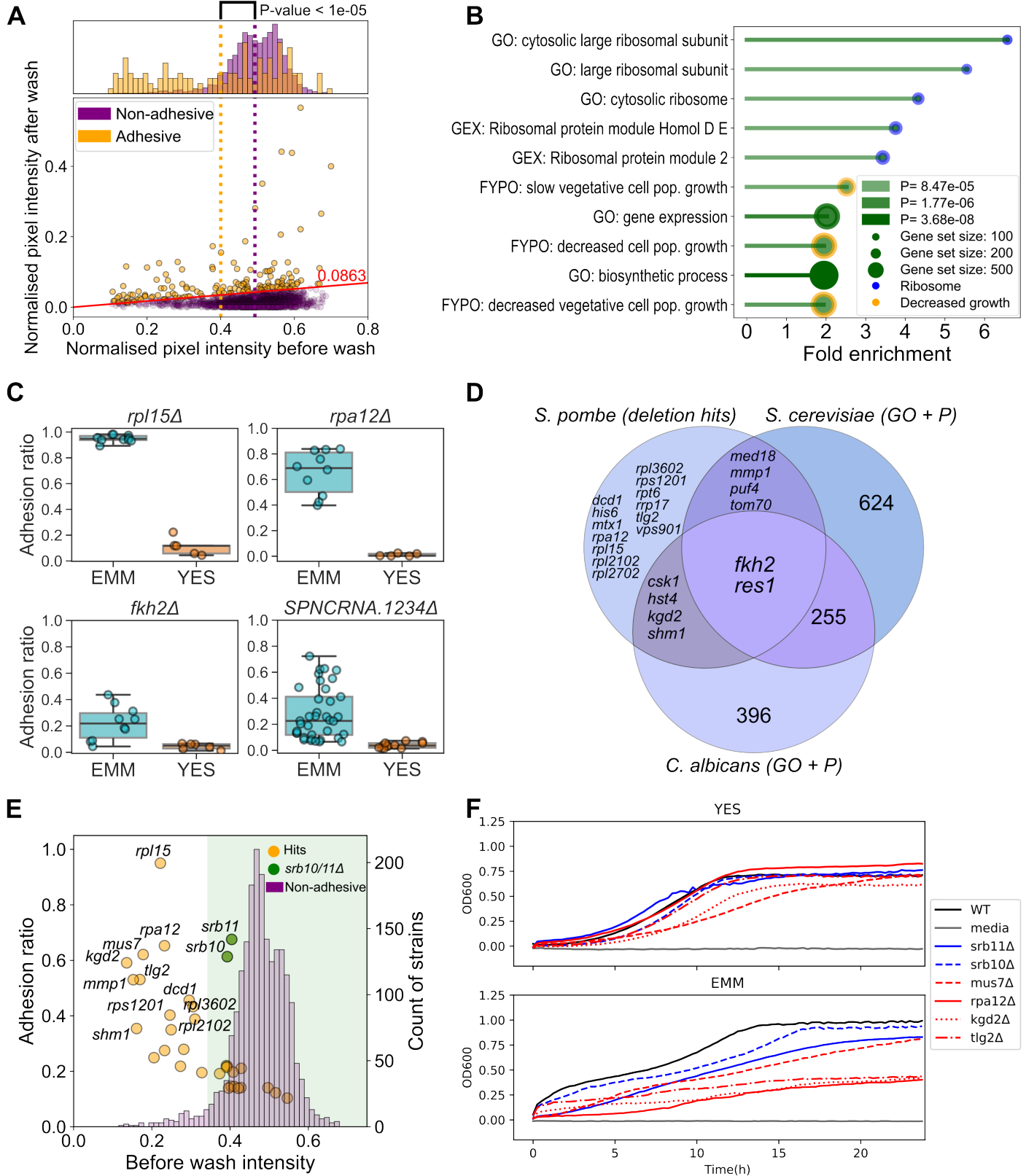


Figure 5: Deletion library screen identified 31 genes associated with MLP formation on minimal media. (A) Scatter plot of mean cell densities before and after washing. Each dot represents a deletion strain, and colours represent adhesive and non-adhesive strains as indicated. The

red line represents the cut-off at the 95th percentile of adhesion values (Supp Fig 10B). The histogram shows the distribution of cell densities before washing as a proxy for growth. The dotted orange and purple lines mark the mean pre-wash intensity values for the two populations. The P-value was determined using a permutation-based T-test with 1E+5 permutations. (B) Bar plot showing fold enrichment for the top 10 most significantly enriched processes from AnGeLi (74). Blue circles indicate terms associated with ribosomes, and orange circles indicate terms associated with decreased growth. Gene sets were sorted based on P-values, with increasing colour intensity representing increasing $-\log_{10}(P\text{-value})$. The size of the circle at the end of each bar represents the size of the gene set. GEX: Gene expression; pop.: population. (C) Box plots of adhesion ratios obtained with the washing assay for 4 of the 31 verified hits (*rpl15Δ*, *rpa12Δ*, *fkh2Δ*, *SPNCRNA.1234Δ*) on EMM (light blue) vs YES (orange). Each dot is an independent observation. Remaining hits are shown in Supp Fig 11. (D) Venn diagram showing functional conservation of the genetically conserved hits from our screen. The hits *SPAC607.02c*, *sre2*, *meu27*, *for3* are not shown as they are not genetically conserved (only present in *S. pombe*). Only *fkh2* and *res1* are also annotated as being involved in MLP formation in *S. cerevisiae* and *C. albicans*. Annotations are assigned using both GO and Phenotype data (GO+P). (E) Scatter plot of adhesion ratios and before-wash colony intensities overlaid by a histogram showing before-wash colony intensities of non-adhesive deletion strains, which were assayed in the middle 60 spots during the original screen. The green-shaded area marks strains that are above the lowest 5th percentile of before-wash colony intensity in the non-adhesive strains, a proxy for growth rate. The *srp10/11Δ* strains, highlighted in green, are the most adhesive strains among those with growth values above the lowest 5th percentile. (F) Line plot of growth measurements (OD600) from WT (JB22), empty media, *srp11Δ*, *srp10Δ*, *mus7Δ*, *rpa12Δ*, *kgd2Δ* and *tlg2Δ* strains in EMM and YES.

Figure 6

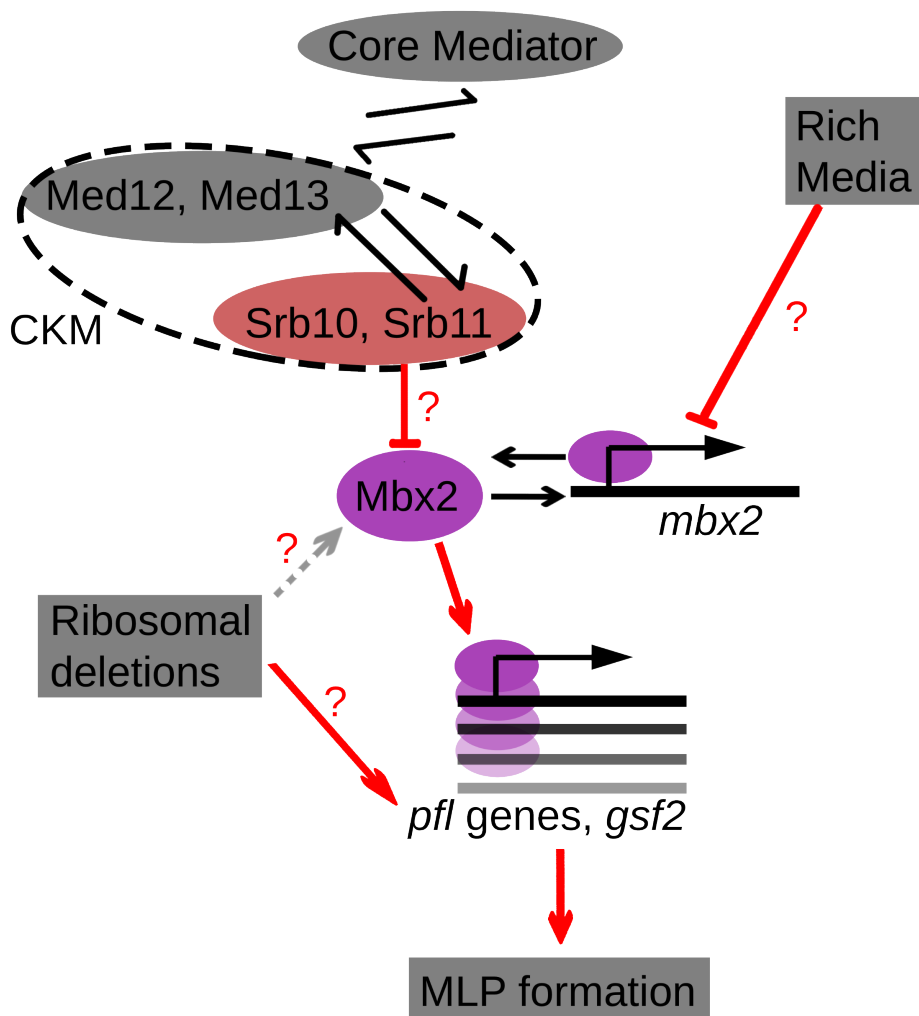
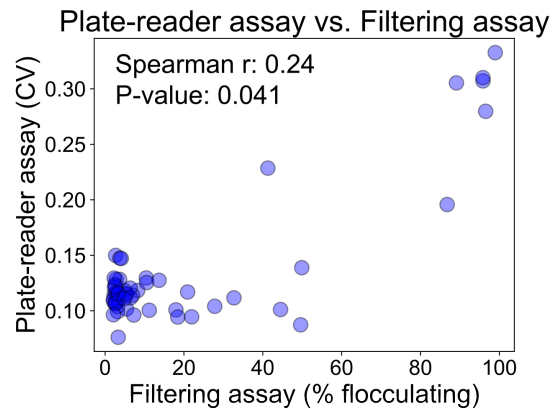


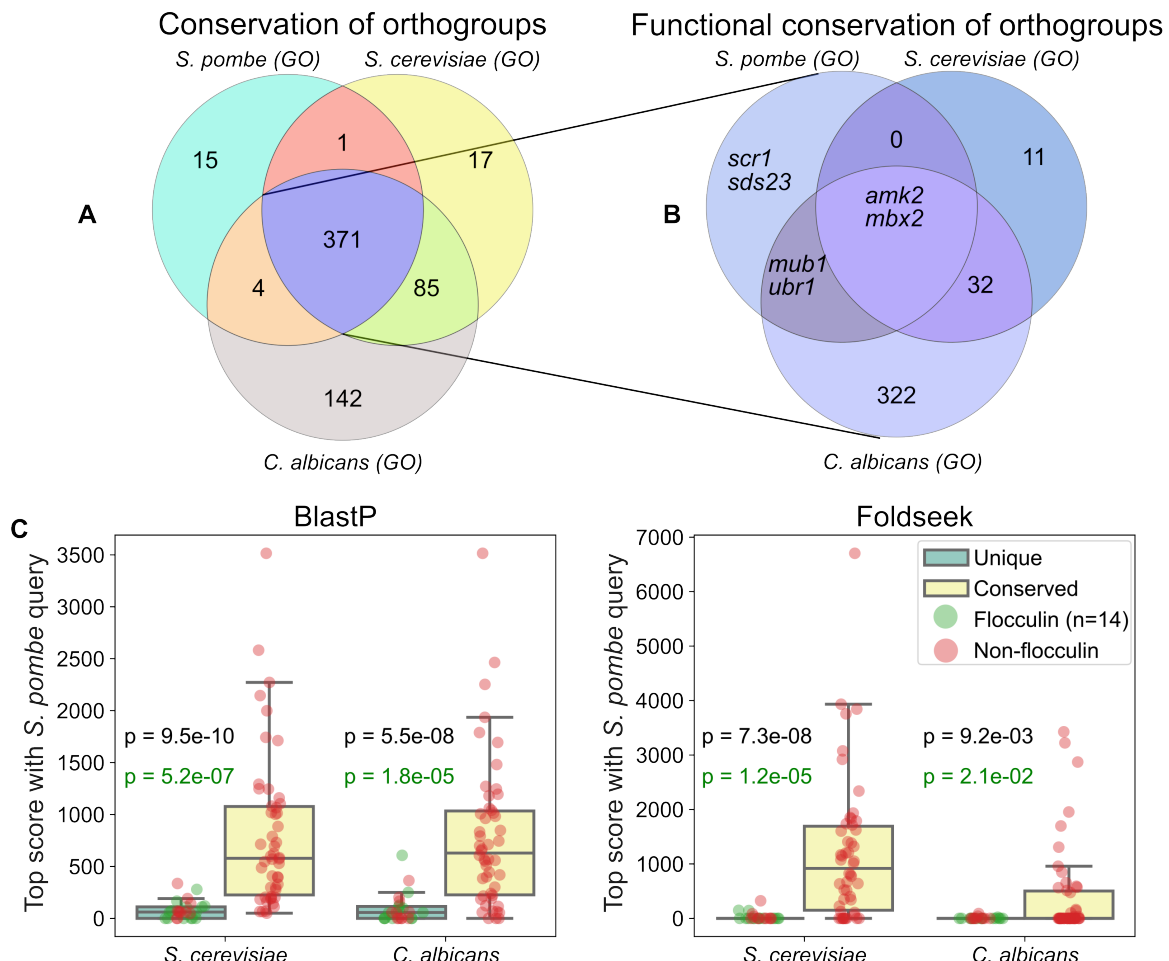
Figure 6: Model for EMM-dependent MLP formation of CKM mutants. We propose that the CKM phosphorylates Mbx2 and targets it for degradation, based on similar observations in *C. albicans* (88) and *S. cerevisiae* (90). Additionally, *mbx2* expression is repressed through an unknown mechanism in YES, as we observed using RT-qPCR. In minimal media, if members of the CKM are deleted, *mbx2* becomes upregulated, triggering the expression of flocculin genes, which in turn cause MLP formation. Deletion of ribosomal genes also triggers MLP formation, although it is unclear whether this occurs through upregulation of *mbx2* or directly through the flocculin genes. The red arrows indicate our main findings, and the red question marks highlight the main outstanding mechanistic questions. See main text for details.

Supplementary Figure 1



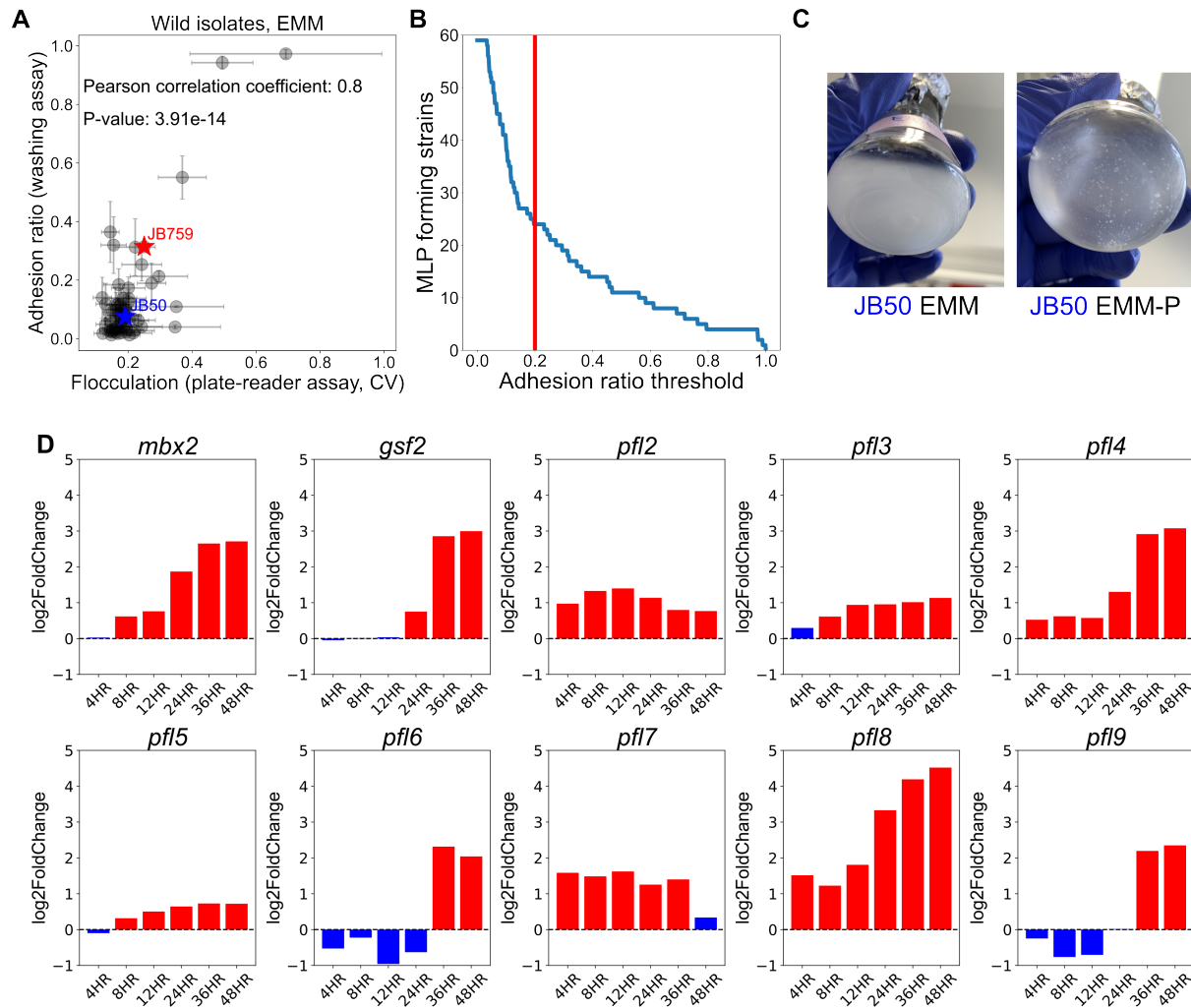
Supplementary Figure 1: Plate-reader assay and filtering assay for flocculation are correlated. Scatter plot comparison of flocculation for the JB50-JB759 segregant library by measuring each strain with a conventional filtering assay (x-axis, n=3) and our high-throughput plate-reader assay which measures the CV of OD600 within each well (y-axis, n=5) (Methods). Each point represents the mean flocculation values for a strain. P-value was obtained with a one-tailed test on whether the Spearman correlation coefficient is larger than 0.

Supplementary Figure 2



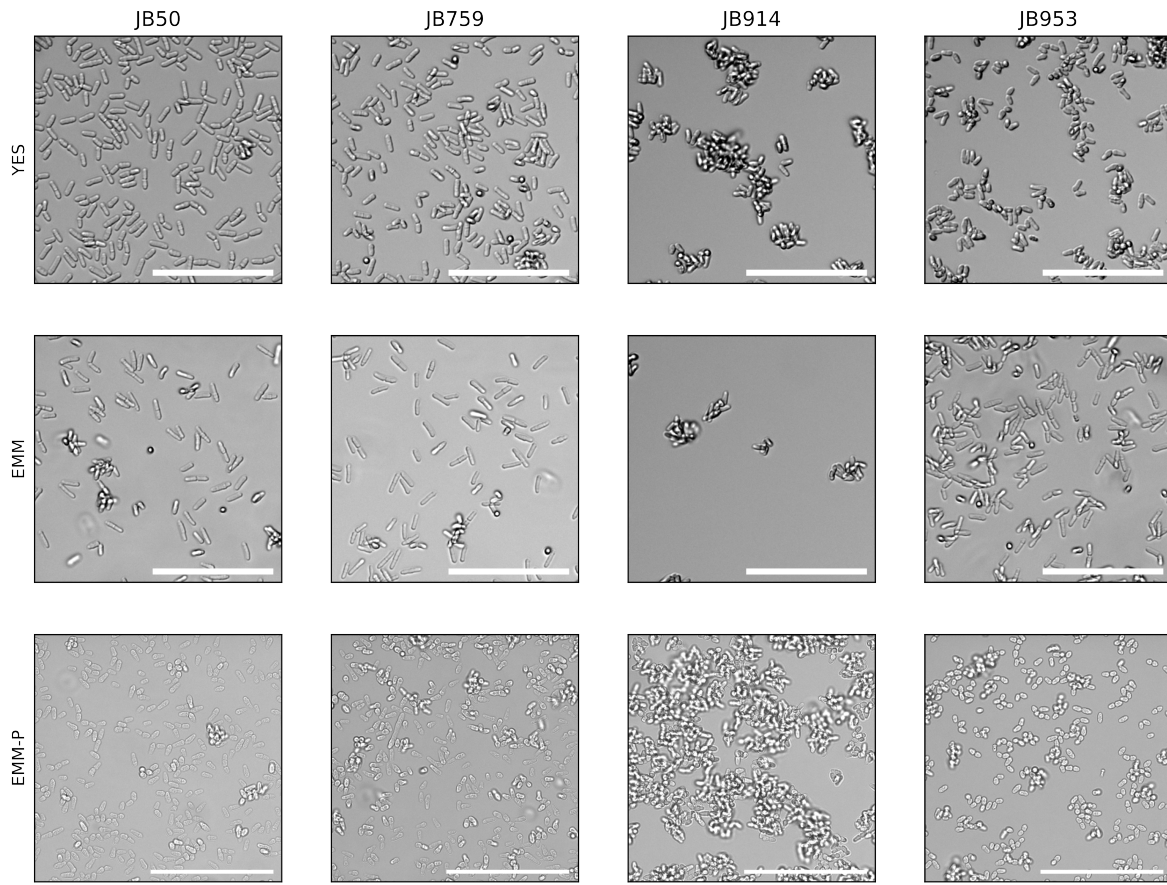
Supplementary Figure 2: Conservation of MLP-related orthogroups between *S. pombe*, *S. cerevisiae* and *C. albicans*. (A) Venn diagram representing genetic and (B) functional conservation of orthogroups between the three species using data only from GO-terms. (C) Highest alignment scores for either 25 protein sequences annotated as unique to *S. pombe* or 50 random conserved sequences using either BLAST-P or Foldseek to identify similar proteins in the *S. cerevisiae* or *C. albicans* proteome (Methods). Each dot represents the highest score using the indicated search algorithm for a given protein. P-values were derived from Mann-Whitney U tests comparing top scores for conserved proteins with either all unique proteins (black) or just unique *S. pombe* flocculins (green).

Supplementary Figure 3



Supplementary Figure 3: Further analysis on adhesion phenotypes of the natural isolates across different conditions. (A) Scatter plot comparison of flocculation and adhesion for the natural isolate library by measuring each strain with a high-throughput plate-reader assay (x-axis, n=11) and our high-throughput adhesion assay (y-axis, n=10). Each point represents the mean values for a strain with the standard error of the mean as error bars. Stars mark JB759 (red) and the lab strain JB50 (blue). (B) Elbow plot of the number of strains designated as “MLP-forming” in at least one condition (y-axis) given different cut-off thresholds (x-axis). Empirically we found that 0.2 sits in the elbow of the plot, suggesting that it is a reasonable cut-off. (C) Phosphate starvation induces MLP formation in the lab strain JB50. Images of the JB50 strain growing in 25ml flasks with 10ml media of either EMM (left) or EMM-P (right). Strains were first grown up on YES plates and then transferred to liquid cultures. There are clearly visible flocs forming in EMM-P. (D) Bar plot of log2FC in gene expression during 2 days of phosphate starvation for selected genes, including the transcription factor mbx2 and various flocculins. Data from (81). Red bars represent significant log2FC values.

Supplementary Figure 4

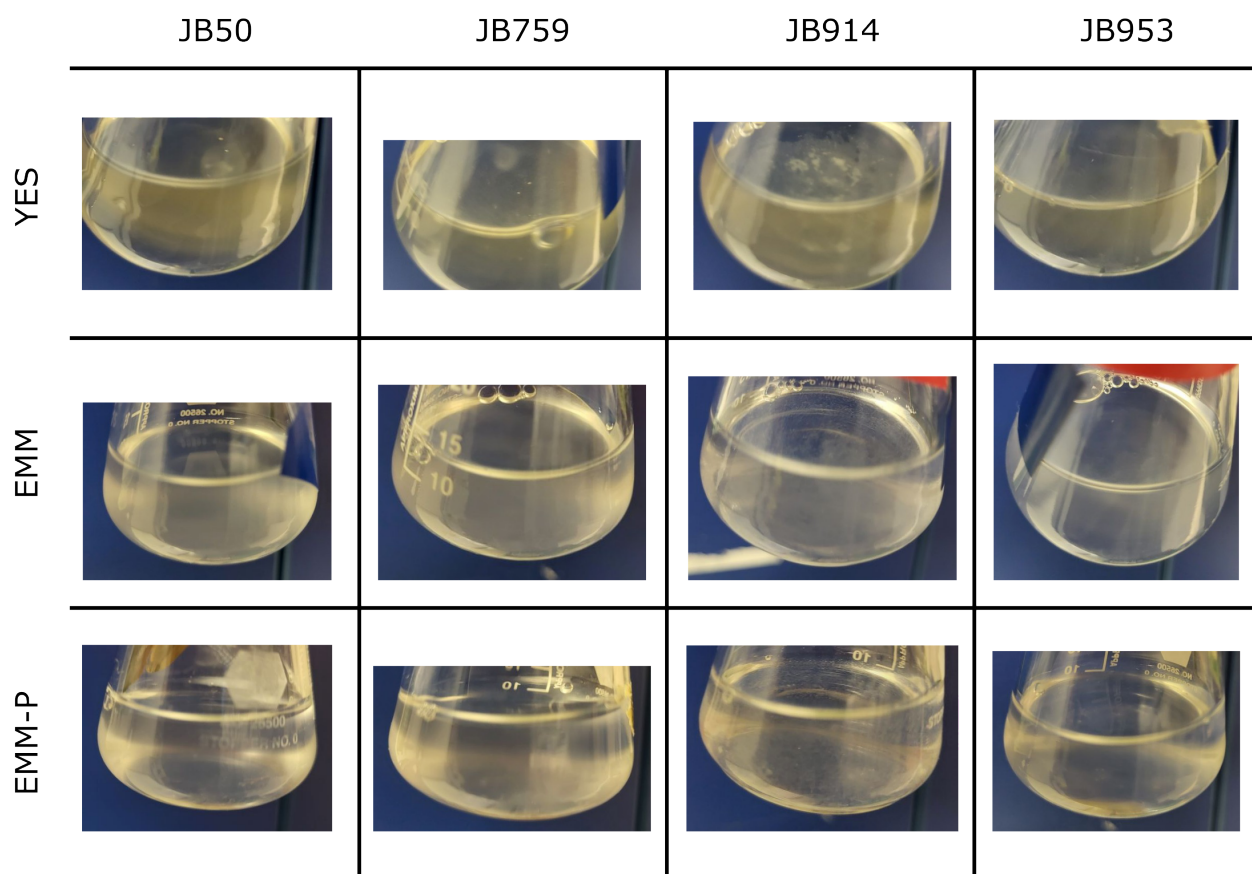


Supplementary Figure 4: Microscope images of wild isolates exhibiting MLPs. Images of during exponential growth of JB50 (lab strain) and three wild isolates (JB759, JB914, and JB953) in media conditions under which they exhibit MLPs. Note: EMM-P images were taken with a 20x objective with 1x zoom, while EMM and YES images were taken with a 5x objective and 2x optical zoom. Images were scaled to be comparable. The images of JB914 and JB953 in EMM and YES are duplicated from this panel and also included in Figure 2. Scale bars are 100 μ m.

Supplementary Figure 5

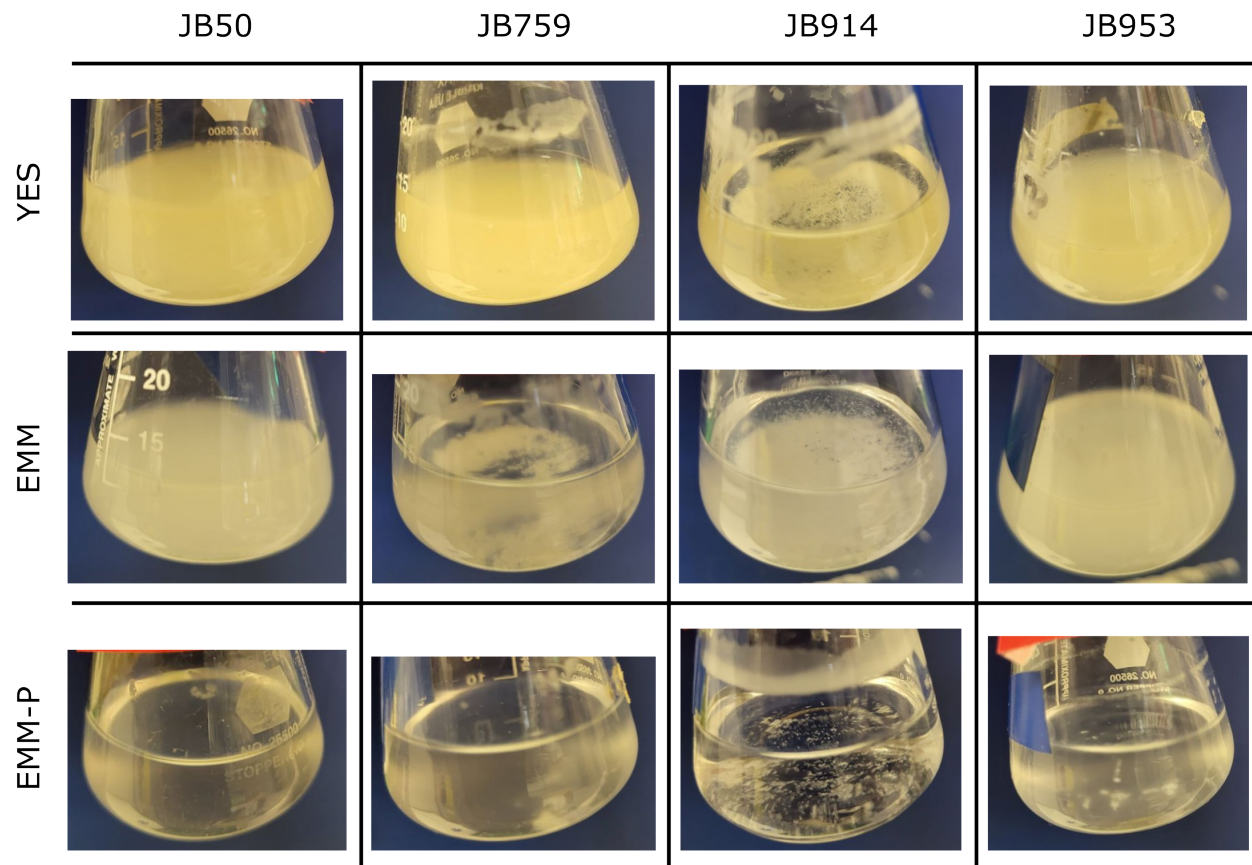
A

Exponential Growth



B

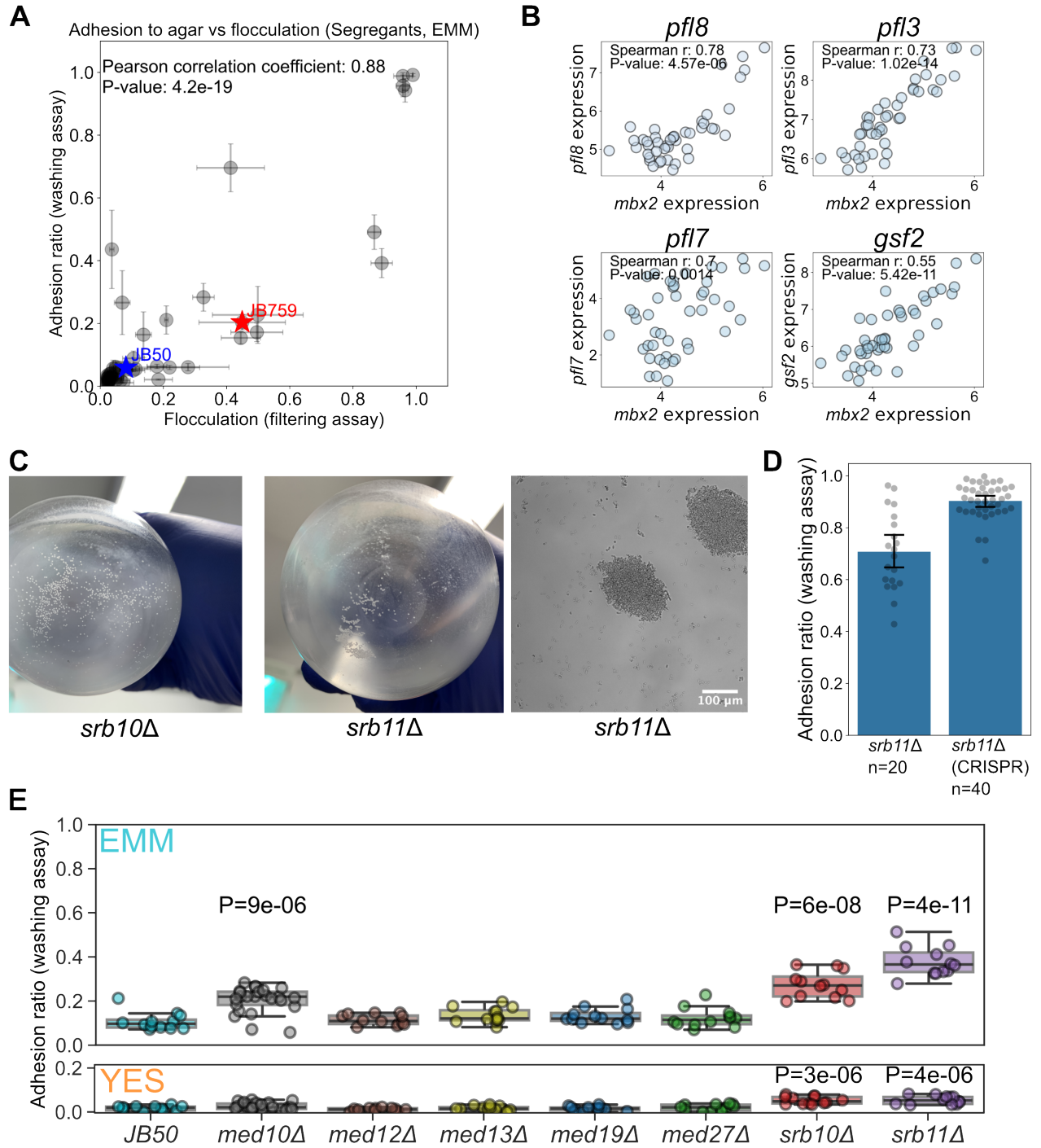
2 Day Cultures



Supplementary Figure 5: Culture flask images of wild isolates exhibiting MLPs. Images of during (A) exponential growth and (B) in saturated cultures after two days of JB50 (lab strain) and three wild isolates (JB759, JB914, and JB953) in media conditions under which they exhibit

MLPs.

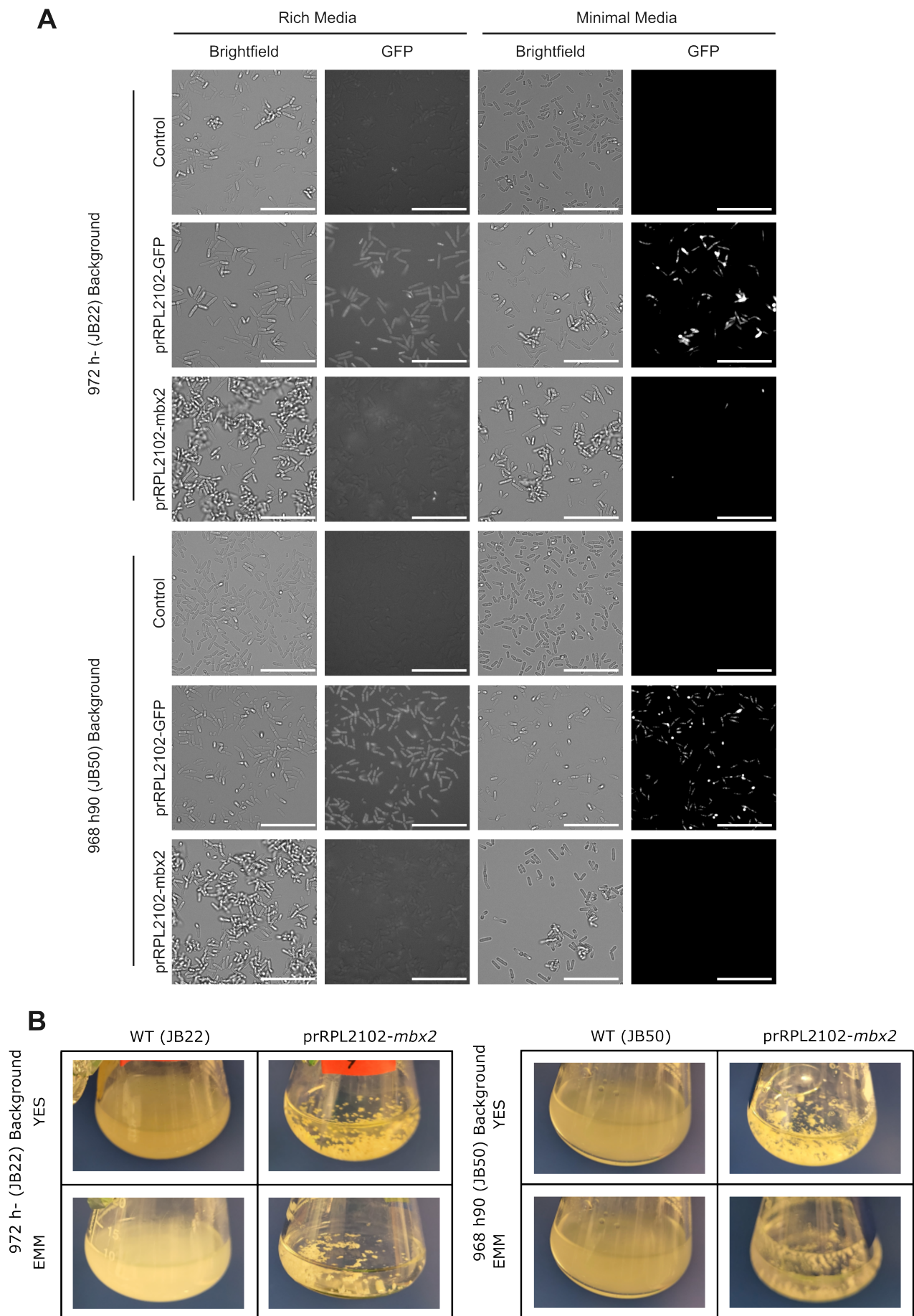
Supplementary Figure 6



Supplementary Figure 6: MLP formation in *S. pombe* involves *mbx2* and CKM components. (A) Scatter plot comparison of flocculation and adhesion for the JB50-JB759 library by measuring each strain with the filtering assay (x-axis, n=3) and the high-throughput adhesion assay

(y-axis, n=10). Each point represents the mean values for a strain with the standard error of the mean as error bars. Stars mark the two parental strains JB759 (red) and JB50 (blue). There is a strong correlation between the two MLPs. (B) Scatter plot of expression levels of four flocculin genes against *mbx2* expression in the JB50-JB759 segregant library (data from (49)), demonstrating a strong association. (C) (Left) Images showing flocculating cultures of *srp10* and *srp11* in 250ml flasks grown in EMM. (Right) Representative microscopy image of *srp11Δ::Kan* (D) Barplot of adhesion values showing that the Kan deletion of *srp11* found in the deletion library phenocopies the CRISPR deletion of *srp11*. Each dot is an independent measurement. Error bars represent the 95% confidence interval for the mean. (E) Box plot showing adhesion values from validation cohort of fresh Mediator gene deletion strains on EMM and YES as indicated. Each dot represents a replicate.

Supplementary Figure 7

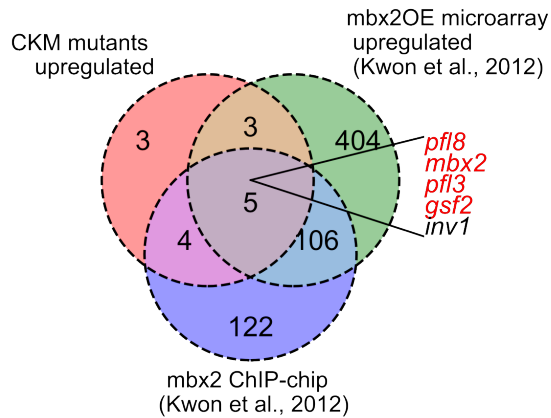


Supplementary Figure 7: Overexpression of *mbx2* drives MLP formation. (A) Microscopy and (B) flask images illustrating the effects of *mbx2* overexpression on cells grown in EMM or YES for both the h- (JB22) and h90 (JB50) backgrounds and the h90 JB50 background. Flask

images were from overnight cultures, and microscope images were from overnight cultures after dilution into fresh media for two hours. The flask images of prRPL2102-mbx2 (JB22) are duplicated and also shown in Figure 3. Scale bars are 75 μ m.

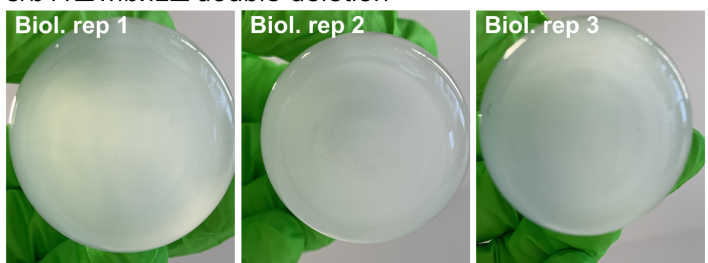
Supplementary Figure 8

A

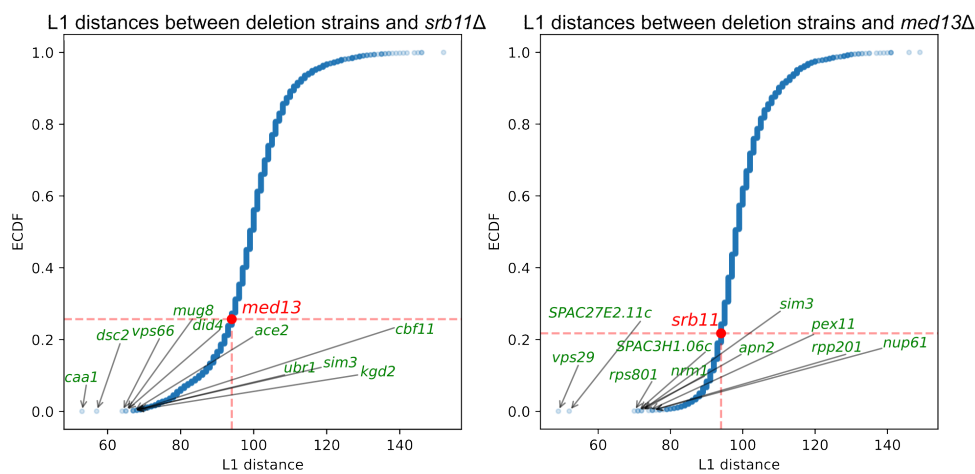


B

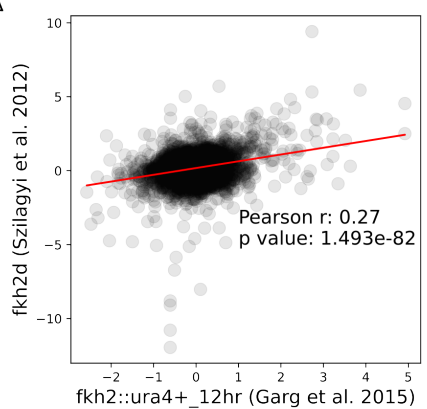
srbl1Δ mbx2Δ double deletion



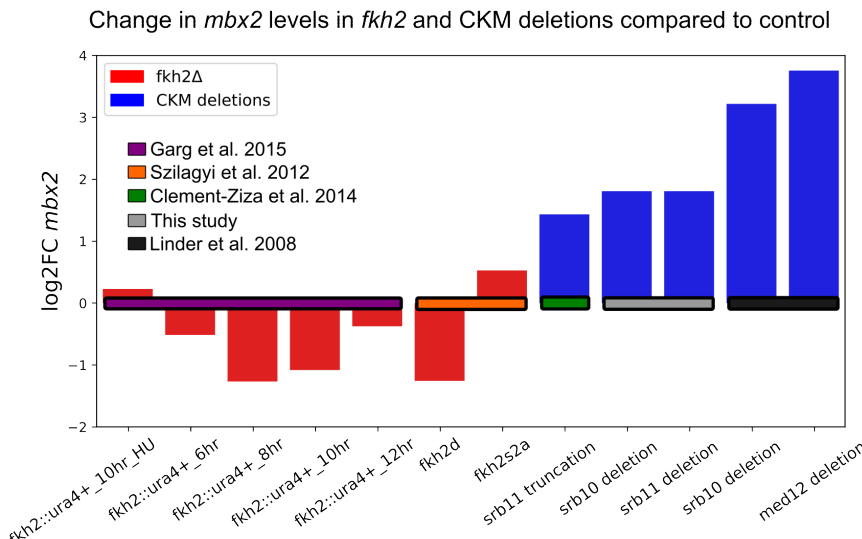
C



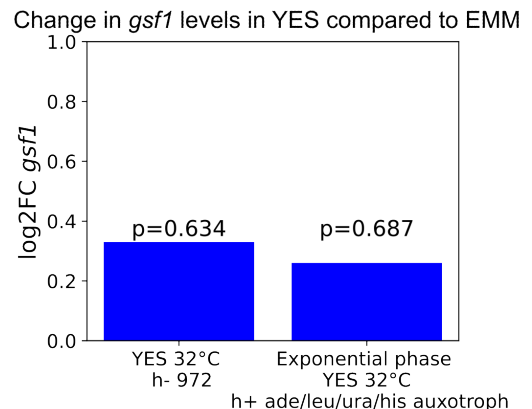
D



E



F

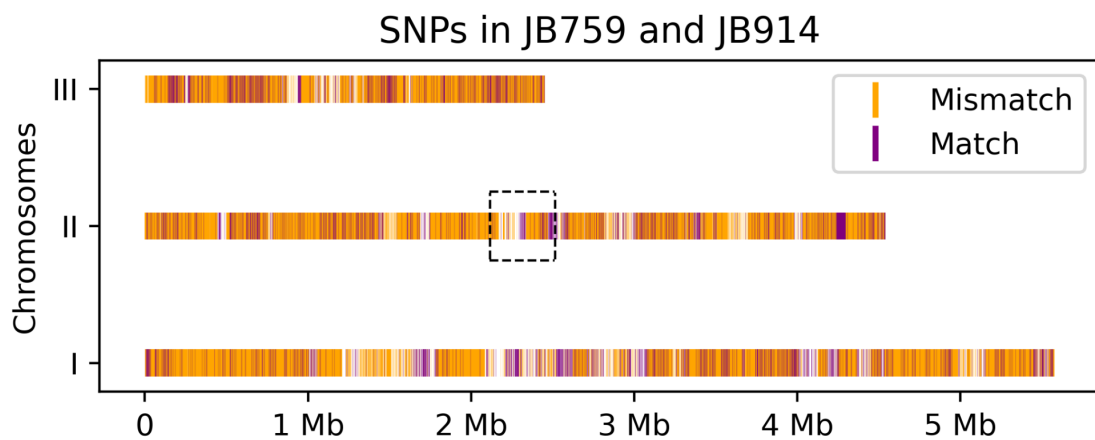


Supplementary Figure 8: Mbx2 drives MLP formation in the *srbl1Δ* strain. (A) Venn diagram showing the intersection of three gene sets: (i) Genes upregulated in CKM mutants, meaning upregulated in the *med12Δ* and *srbl10Δ* microarray data from (68) and in the *srbl1* truncated

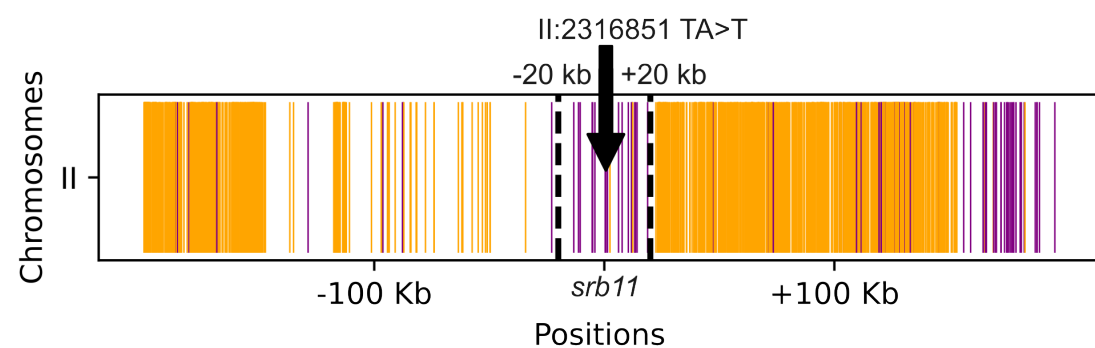
segregant RNA-seq data from (49) (Fig 4E), (ii) Genes upregulated after *mbx2* overexpression obtained from (27) and (iii) Genes bound by *Mbx2* obtained from (27). (B) Images showing non-flocculating cultures of three biological replicates of *srb11/mbx2* double deletion strains. (C) Empirical cumulative distribution function of L1 distances between phenotype vectors for the *srb11 Δ* strain and all other gene deletion strains for growth phenotypes across 131 different conditions. For each condition in each strain, a number of -1, 0, or 1 was assigned to denote sensitivity, neutrality and resistance, and the L1 distance is the sum of the absolute value of the differences across all phenotypes as measured in (96). The 10 deletion strains closest in their phenotypes to *srb11 Δ* and *med13 Δ* are highlighted on the plot. The similarity score of *med13 Δ* is in the 21st percentile. (D) Scatter plot of fold changes comparing two different data sources for transcriptomic changes upon *fkh2* deletion. Dots mark individual genes in the datasets, while the line of best fit is shown in red. This plot concludes that it is fair to use the two data sources to draw joint conclusions from them. (E) Bar plot showing log2 fold-changes in *mbx2* expression levels from experiments in which *fkh2* was deleted (red) and in which CKM subunits are deleted (blue). Selected *fkh2* deletion experiments included microarray data from (86) and (97), while CKM subunit deletion experiments included *med12 Δ* and *srb10 Δ* microarray data from (68), fold change calculated by grouping RNA-seq data from (48) for segregants with the *srb11* truncation vs those without the mutation (Fig 3D), and the RT-qPCR data collected in this work. (F) Bar plot showing log2 fold-changes in *gsf1* expression in YES compared to EMM. There is no significant upregulation in either of the two replicates. Data and P-values were taken from (98).

Supplementary Figure 9

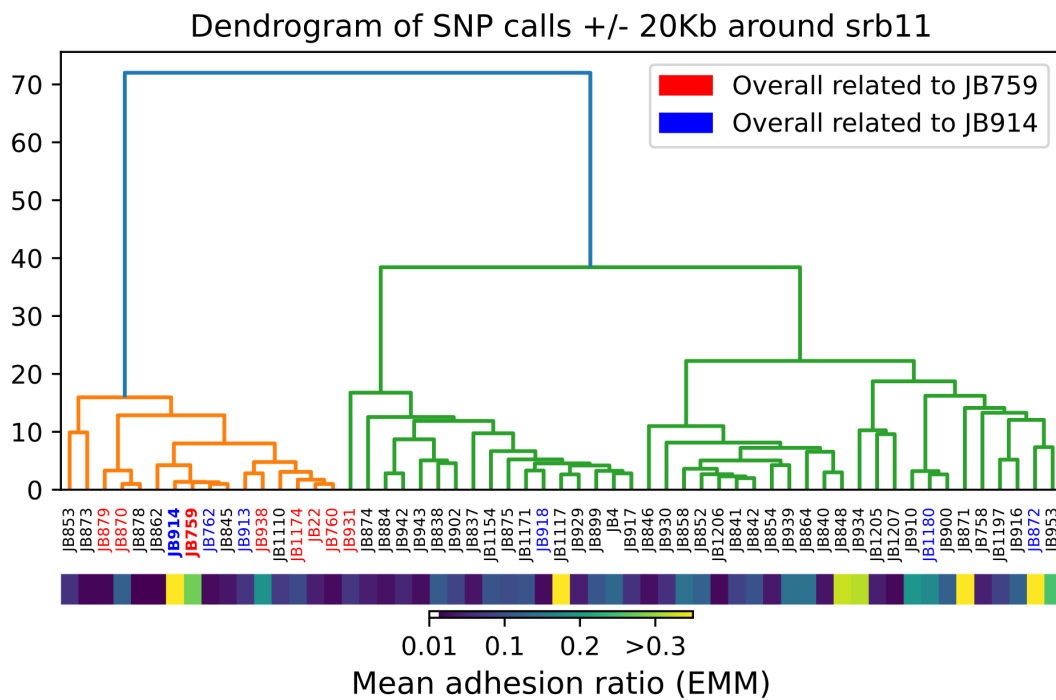
A



B



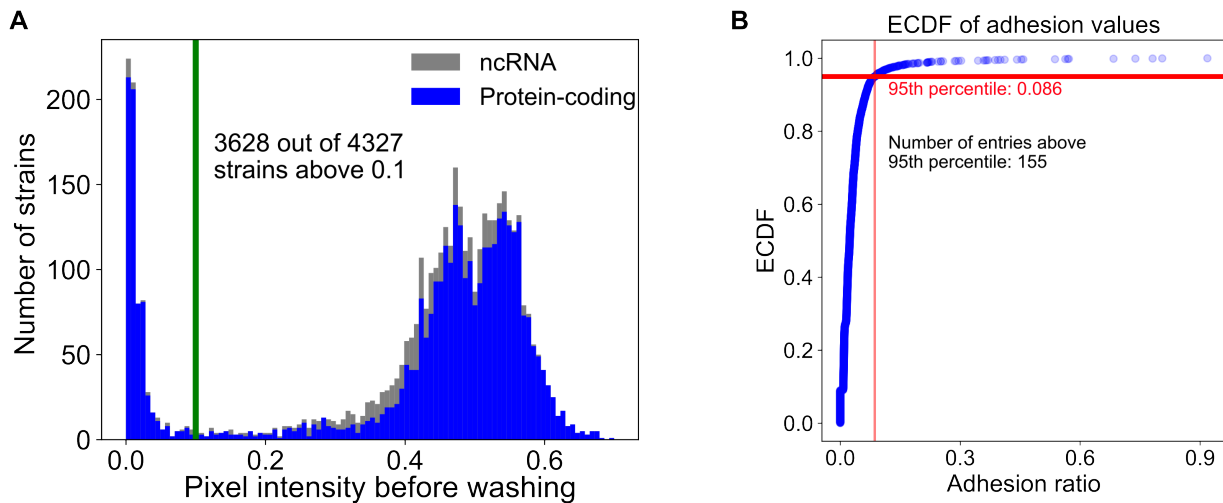
C



Supplementary Figure 9: The srb11 variant is present in the JB759 and JB914 natural isolates, and segregates with MLP-formation across natural isolates closely related to those strains. (A) *S. pombe* reference genome visualised for each of the three chromosomes, with vertical

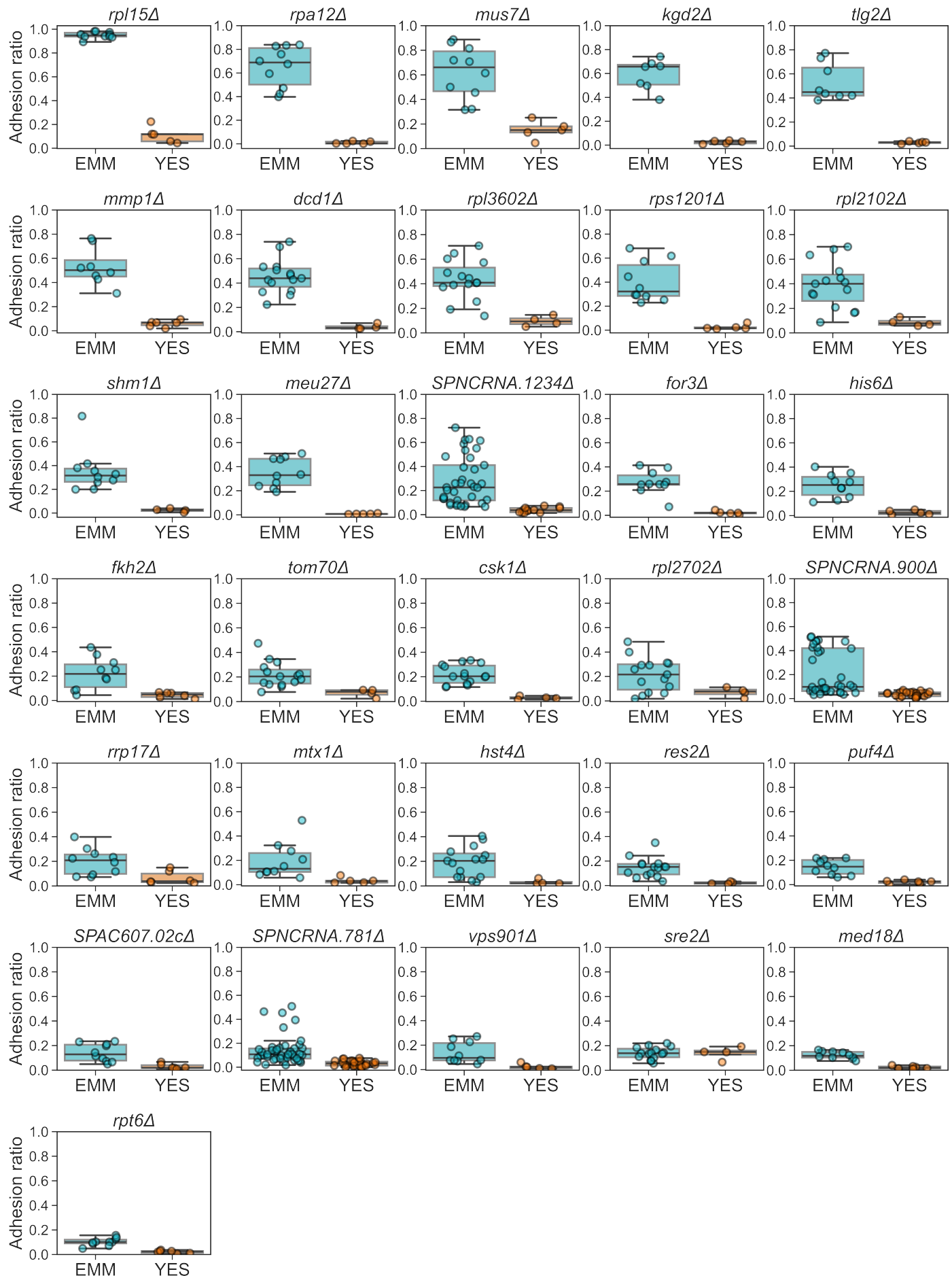
lines marking variant loci (called in (45)) compared to the reference genome in at least one of the two strains. Variant loci with the same alternative allele for JB759 and JB914 are marked with purple, while variant loci where alleles do not match are marked with orange. (B) Inset showing the region surrounding the causal *srp11* variant. The +/- 20Kb window is highlighted. Vertical lines indicate variant alleles as in A. (C) Dendrogram illustrating genomic similarity of natural isolates based on the +/- 20Kb window around the *srp11* frameshift mutation. Red text indicates strains closely related to JB759 considering the whole genome (based on (45)), while blue text indicates strains related to JB914. Heatmap below indicates adhesion ratio in EMM.

Supplementary Figure 10



Supplementary Figure 10: Deletion library screen for MLP formation on EMM. (A) Histogram showing cell densities, measured by inverse pixel intensity after 4 days of growth, for strains in our deletion library screen before washing. (B) Empirical cumulative distribution function (ECDF) of adhesion ratios from the deletion library screen, with red lines showing the cut-off for the 95th percentile. Strains above the cut-off were used for enrichment analysis.

Supplementary Figure 11

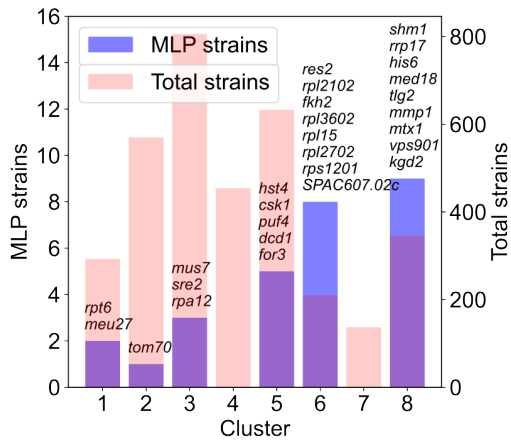


Supplementary Figure 11: Verified hits from the deletion library screen for MLP formation, assayed both on EMM and YES. Box plots of adhesion ratios obtained with the washing assay for the 31 high-confidence hits on EMM (light blue) vs YES (orange). Each dot is an

independent observation. Adhesion was generally specific to EMM, except in the case of *sre2Δ*. The images of *rpl15Δ*, *rpa12Δ*, *fkh2Δ*, *SPNCRNA.1234Δ* are duplicated from this panel and also included in Figure 5.

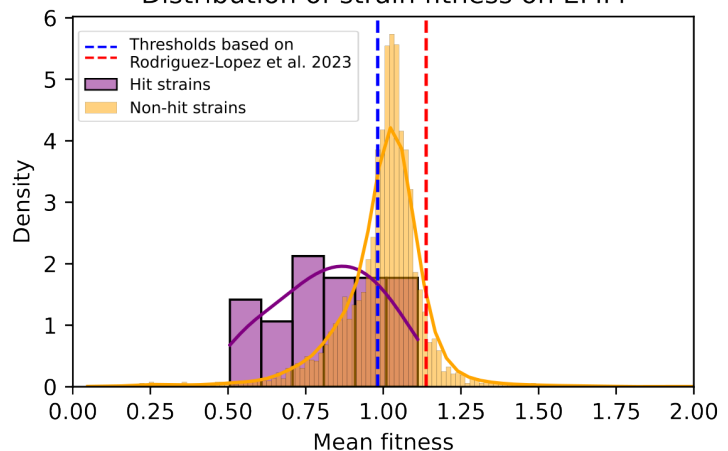
Supplementary Figure 12

A



B

Distribution of strain fitness on EMM



Supplementary Figure 12: MLP-forming hits belong in various phenotypic clusters, but generally exhibit slow growth. (A) Bar plot showing the number of MLP-forming (blue, left axis scale) and total (blue, right axis scale) strains in each broad phenotypic cluster of deletion strains identified in (96). (B) Histogram of mean fitness values, based on growth in solid EMM media, for each strain as defined in (96). MLP-forming hit strains are shown in purple, and all other strains are in yellow. Blue and red dotted lines show the thresholds beyond which strains were defined as slow- or fast-growing, respectively.